Co-published by
Institute of Fluid-Flow Machinery
Polish Academy of Sciences
Committee on Thermodynamics and Combustion
Polish Academy of Sciences

http://www.imp.gda.pl/archives-of-thermodynamics/

Experimental investigation of inside zigzag pipe collector solar air heaters: energy and exergy analyses

Murat Kaya

Hitit University Mechanical Engineering, Çorum 1900, Turkey
Author email: mrtkaya@hotmail.com

Received: 06.09.2023; revised: 12.09.20243; accepted: 09.10.2024

Abstract

In this study, collectors with two different designs as solar air heaters were examined. Both collectors have equal dimensions and panels with the same features are placed inside. A zigzag strip is placed within the cavities of the collector I panel. The inside of the cavities of the collector II panel is left empty. The thermal efficiency of the panel was observed by providing air flow from the bottom of both collectors. A good design is essential for an efficient collector. As a result of the studies carried out, according to the second law of thermodynamics, the efficiency of collector I, which has a zigzag inside the panel, is between 20.2% and 38.8%, whereas the efficiency of collector II, which is hollow inside the panel, varies between 17% and 32.2%.

Keywords: Solar air heating; First law of thermodynamics; Second law of thermodynamics; Exergy; Collector efficiency

Vol. 45(2024), No. 4, 215–222; doi: 10.24425/ather.2024.152011

Cite this manuscript as: Kaya, M. (2024). Experimental investigation of inside zigzag pipe collector solar air heaters: energy and exergy analyses. *Archives of Thermodynamics*, 45(4), 215–222.

1. Introduction

Turkey obtains most of its fossil-based energy from foreign countries. A large amount of this energy is used for heating purposes in industry, workplaces and homes. Foreign dependency on energy use is quite high. However, in terms of renewable resources, it is in a position to benefit greatly from solar energy, especially in terms of its location in the world. In the drying of grain products, healthier and more efficient grain drying can be done by using solar energy instead of traditional methods. In this respect, it has a remarkable potential.

Solar energy is energy that has no fuel costs. Many studies have been carried out to benefit more from this energy. Many scientific studies have been conducted on collectors of different designs to determine the greater efficiency of such systems. In these works, the use of flat sheet panels is generally common. Different types of solar radiation air heat exchangers are produced by adding various geometrically shaped parts into these panels to increase the heat transfer rate. Solar air heated collectors have many advantages. Easy and clean energy can be obtained, there is no fuel cost, and it is easy to produce locally. Small volumes can be heated, and some leaf-type plants can be dried. For this reason, different designs have been developed recently to make collectors more efficient.

Abene et al. [1] designed two types of collectors for drying grapes. They placed various obstacle particles in rows within the collector panel and examined the increase in thermal efficiency. They compared collector WDL1 (waisted delta lengthways) and collector WO (without obstacles), which they designed. At a certain airflow rate, the thermal efficiency of the WDL1 col-

Nomenclature

A_{col} – absorber area of the collector, m^2
c_p – specific heat capacity at constant prerssure, kJ/(kg K)
$\dot{E}_x$ – dimensionless inlet exergy flow
$\dot{Q}$ – heat rate, kW
h – enthalpy, kJ/kg
I_T – solar radiation, W/m^2
$\dot{m}$ – fluid mass flow rate, kg/s
P – pressure, Pa
R – ideal gas constant, kJ/(kg K)
Re – Reynolds number
s – entropy, kJ/(kg K)
$\dot{S}$ – entropy production, kJ/(kg K s)
T – temperature, K

Greek symbols

α – absorption factor of the solar receiver
ε – specific exergy, kJ/kg
η – thermal efficiency
τ – effective transmission
ψ – exergy efficiency

Subscripts

air – air
col – collector
gen – generation
in – inlet
out – outlet
o – ambient
r – radiation

lector was 25% and 23%, respectively. In the WO heat collector, it was 29% and 24%.

Zima et al. [2] simulated the transient processes occurring in liquid flat-plate solar collector tubes using a one-dimensional mathematical model. Boundary conditions were assumed as time dependent. Differential equations were derived under boundary conditions and operating conditions, and the equations were solved using the finite difference method.

In the study of Krawczyk [3], sewage sludge from a wastewater treatment plant in Błonie near Warsaw was examined in 2012. This mud is dried with solar energy. Experimental evidence is presented in the study that there is a relationship between the cumulative drying potential of ventilation air and the condition of dried sludge. The amount of water evaporated from the dried sludge mass was determined. They determined the weight values in three groups based on the initial unitary mass. These values are between 5 and 8.3 kg/m^2 in group I, between 8.3 and 12.5 kg/m^2 in group II, and between 12.5 and 20 kg/m^2 in group III.

Khatri, R. et al. [4] in their experimental study, investigated the performance of a solar air heater with an absorber plate made of aluminium material with perforated cylindrical wing geometry. They applied the liquid at three different speeds. In measurements made on the wing-arched wavy absorber plate at a flow rate of 5 m/s, the best performance was measured in the temperature range of 55–70 °C.

Khawajah et al [5] studied 2-fin, 4-fin and 6-fin double-pass solar air heater. Instead of absorber plates, layers of wire mesh were placed between the wings. The mass flow rate was in the range of 0.0121–0.042 kg/s. The maximum efficiency was determined as 75.0%, 82.1% and 85.9%, respectively, for the 2, 4, 6 fin solar air heaters when the flow rate was 0.042 kg/s. The temperature difference ΔT was greater in the 6 fin solar air heater than in the 2 and 4 fin solar air heaters. The peak ΔT was 43.1 °C and 62.1 °C, respectively, when the mass flow rate was 0.0121 kg/s in a 6 fin solar air heater.

Sachın et al. [6] conducted solar air heater experiments on six different roughened surfaces. The air flow on rough surfaces – transverse, pit, side curved, spring, and sine wave surfaces was examined. Experiments were carried out in a wide range of Reynolds numbers (Re). They achieved the best result for a sine wave surface at Re = 15 000.

Petela [7] assumed that the energy of the atmosphere was infinite and its exergy was zero. Solar air heaters get their energy directly from the atmosphere. The exergy entering the air heaters is the exergy of E_x from solar radiation alone. Derivation procedures for three radiation categories are discussed in the study. A closed system, black flux and any arbitrary radiation flux were studied. Formulas have been created for the conversion of radiation into work or heat.

In the work of Sıvakumar et al. [8], the transformation, quality and irreversibility of the energy in the systems are determined more clearly by exergy analysis. By comparing the theoretical values of cumulative efficiency, energy efficiency and exergy efficiency, it was found that taking into account the heat capacities of the glass cover and panel gives a higher output in all thermal models.

Farahat et al. [9] determined the exergy efficiency by developing a mathematical model for linear parabolic solar collectors.

Çomakli et al. [10] conducted the experiment in February, March, April, May, June and July. They made a different plate design inside each of the four different collectors. The highest energy efficiency occurred when a distorted roughened surface was made between the absorber plate and the back plate.

Karsli [11] designed four different air-heated solar collectors. The experiments were carried out from March to July in Erzurum province in 2004. The first law efficiency varied between 26% and 80% for collector I, between 26% and 42% for collector II, between 70% and 60% for collector III, and between 26% and 64% for collector IV. The second law efficiency values varied between 0.27 and 0.64 for all collectors.

Altfeld et al. [12] studied how much the total surface area properties of the collectors affect the energy efficiency. It has been determined that the exergy efficiency is better when the collector surface is enlarged and the air flow is reduced.

Altfeld et al. [13] used different types of designed collectors in their studies. The collectors were examined for high heat and low friction losses. They determined the net input and output exergy values of solar collectors. They concluded that it is not appropriate to have a high density of rough surface fins attached to the panel surfaces inside the collector.

In their study, Gupta et al. [14] determined the exergy efficiency of solar air heater systems having various parameters such as the aspect ratio of the collector, the mass flow rate per unit area of the collector plate and the channel depth of the plate.

2. Experimental setup and measured values

In this study, two different collectors with solar air heating were designed and installed in the city of Çorum, Turkey – 39:14 North latitude; at 38:27 East longitude. The surface of the collectors is fixedly facing the sun at 12 o'clock. The collector surface was adjusted according to the azimuth angle of the sun.

The system was designed as composed of two different collectors. The collectors were manufactured from two metal sheets, on which half circle grooves were formed. Then, these metal sheets were placed upon each other in such a way that circle channels were formed. The diameter of each groove was 6 cm. In the first experiment, zigzag metal parts of 4 cm width were placed along the grooves of panel I. In this application, it was aimed to increase the contact of flowing air and the collector's inner surface in order to improve the heat transfer rate. In the second panel II, grooves were left empty for the flow experiment.

The frame of the collector from outside to outside measures 96 cm × 200 cm × 15 cm and is made of 2 cm thick wood. The glass surface area of the collector (A_{col}) is 0.92 m ×1.96 m = 1.8 m^2. The panels placed inside the collector are designed to measure 90 cm × 180 cm × 0.1 cm and be manufactured from a galvanized metal sheet. The surface area of the two panels is the same ($A_{p1} = A_{p2}$), and is equal to 0.9 m ×1.8 m = 1.62 m^2. Insulation of the panels was assured by installing 5 cm thick glass wool, which was placed between the bottom and side surfaces of the panel. The front surfaces of the panels were covered by glasses that have a thickness of 0.7 cm. As can be seen in Fig. 1, the inner and outer surfaces of the collectors were painted black. A hole of 10 cm diameter was drilled, in order to maintain inflow of the air outside. Then, in order to sustain equal distribution of air to the grooves of the panel, a part that is made of perforated sheet metal was fixed to the edges of groove entrances. The air outside was sucked into the collectors by a fan. The designed solar collector has a glass surface and a corrugated panel placed inside; the cross section profile is shown in Fig. 2. The flow rates of the air flowing through the collectors were equal. The temperature of inflowing air was that of the ambient temperature. The heating surface area (A_{col}) was 1.8 m^2. The collector was placed on a wheeled setup that was made of stainless profile steel. In addition, a special worm screw setup was placed behind the collector frame. According to the azimuth angle of the sun that changes daily and seasonally, the collectors were adjusted with the use of a worm screw for a better exposure angle and better absorption of sunlight. In the experimental study, the energy coming from the sun to the collector surface, the surface temperature, temperature and pressure values of the air entering and leaving the collector were measured.

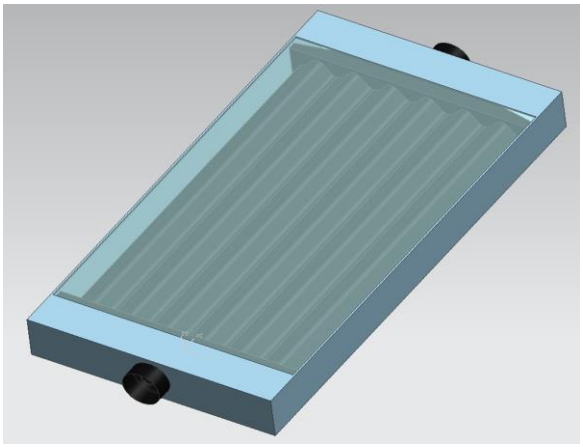

Fig. 1. The panel and collector with zigzags in the grooves.

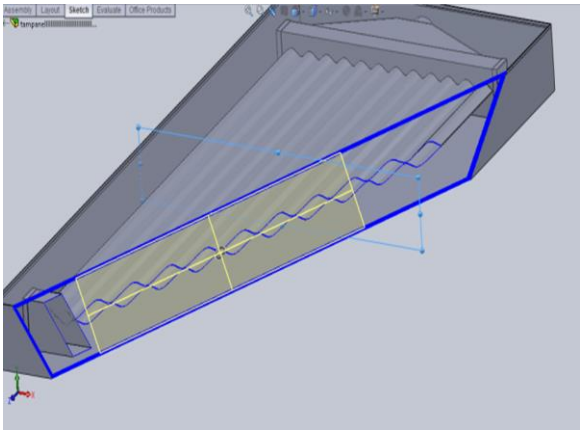

Fig. 2. Air heater heat exchanger cutaway profile.

In order to measure the required values in the experimental system, thermocouples were placed on the collector surface, at the air inlet and outlet points, and at ambient conditions. Thermocouple tips are well attached to the measuring surfaces. Experimental values were measured 30 min after the collector was exposed to the sun. Values were recorded every 30 min. The same time period of 8:30 and 17:00 daily was recorded.

The experimental setup consists of two different plates, as in Fig. 3. The inside of the first plate I is flat and the second plate II is zigzag. The designed solar collector is covered with a flat plate and glass, and the air passing through it is heated. A fan, air valve, pyrometer and multimeter were used to measure the required test results.

3. Energy and exergy analysis

Exergy analysis is a thermodynamic analysis technique based on the second law of thermodynamics. Exergy analysis helps improve and optimize designs and analyses. The authors of [15] stated it is the only analysis to compare systems with their actual values. They examined exergy on two features: (1) how close the actual performance is to the ideal one and (2) more precisely determine from energy analysis the types, causes and locations of thermodynamic losses.

Esen [16] performed the solar collector tests in two stages. In the first stage, he placed different geometrical blocks inside the collector. In the second stage, he presented an energy and exergy analysis in both cases without placing any geometrically shaped blocks. Air flow at different flow rates into the collector is made first over the panel and then under the panel. The author determined the optimum efficiency depending on the heat absorbency of the panels. Bejan [17] and Wark [18] stated that the

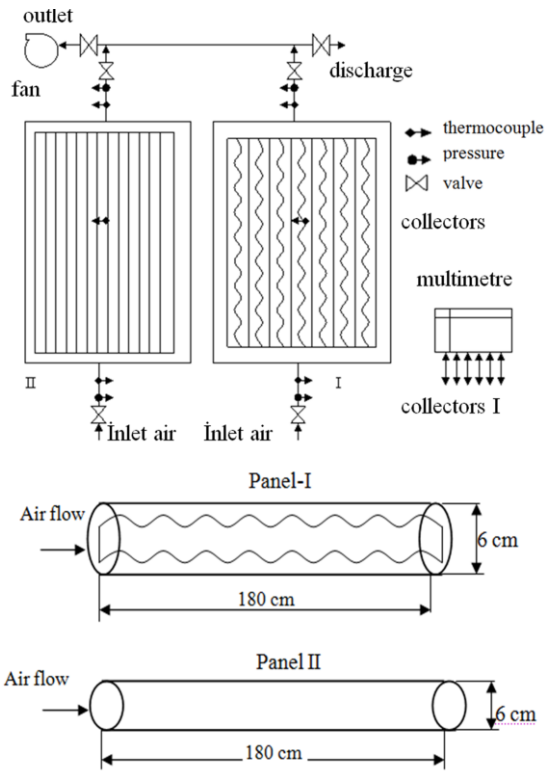

Fig. 3. Experimental setup.

efficiency of collector systems will be determined according to the second law of thermodynamics. They carried out the study firstly with an auxiliary substance method that increases fluid flow, and secondly with the heat transfer method.

In order to use the energies of the systems at the most efficient level, they must be determined clearly [19]. They argued that this could only be possible by applying exergy analysis to systems. The conversion, quality and irreversibility of energy in systems are determined more clearly by exergy analysis. They tested the performance by attaching fins to the plates to increase absorbency.

Table 1. Values adopted for the flat-plate solar collector.

Quantity	Value
Absorber material	Galvanized steel sheet
Absorber plate	0.92 m × 1.96 m
Thickness	0.001 m
Absorptance	0.9
Emittance	0.1
Absorber coating	Dull black paint
Absorptivity of the absorber	$\alpha = 0.65$
Tube external diameter	0.06 m
Tube internal diameter	0.059 m
Reflectivity of the absorber	$\rho = 0.16$
Sealant	Silicon rubber
Back insulation	Glasswool (thickness 0.05 m)
Side insulation	Glasswool (thickness 0.025 m)
Effective product transmittance--absorptance	$\tau\alpha = 0.78$
Panel heat transfer area	$A_{p1} = A_{p2} = 1.62$ m^2
Uncertainty in reading values of table	± 0.1%–0.2%

3.1. Energy analysis

The amount of energy coming to the collector surface due to solar radiation constitutes the thermal energy of the system. The equation that determines the solar energy coming to the solar air heater collector surface is

$$\dot{Q}_{sun} = I_T \tau\alpha A_{col}, \quad (1)$$

where A_{col} is the surface area of the collector corresponding to the sun radiation direction, $\tau\alpha$ gives the solar energy radiation value of the collector surface, A_{col} is the collector area, and $\dot{Q}_{sun}$ is the thermal energy from the sun absorbed depending on the collector surface permeability ability [11,16,20].

Exergy calculations of air entering and exiting the glass-covered solar collector at different flow rates have been made. The amount of useful energy gained by the air flow entering the collector is:

$$\dot{Q}_{air,col} = \dot{m}_{air} c_{p,air} \left(T_{air,out} - T_{air,in}\right). \quad (2)$$

The energy efficiency of the system, according to the first law of thermodynamics, is defined as the ratio of the thermal energy gained by the flow to the radiant energy coming from the sun to the collector surface:

$$\eta = \frac{\dot{m}_{air} c_{p,air} \left(T_{air,out} - T_{air,in}\right)}{I_T \tau\alpha A_{col}}. \quad (3)$$

3.2. Exergy analysis

In many energy systems, exergy analysis is applied to the systems to obtain accurate numerical values. An attempt was made to prove its usability by applying exergy analysis to the systems. It was found that high exergy losses could be reduced by designing efficient solar collectors [8,20–22].

Exergy analysis has been applied to accurately evaluate the thermal energy efficiency of different types of designed solar collector panels. It has been applied to all components of the collectors, including glass cover, sun ray angle, water flow rate and environmental conditions [23,24].

Exergy analysis more clearly determines the transformation, quality and irreversibility of the energy in the systems. However, some assumptions were made initially for solar collectors. The mass balance of solar collectors is:

$$\sum \dot{m}_{in} = \sum \dot{m}_{out}. \quad (4)$$

The exergy flow in the control region is given by Eq. (5):

$$\sum \dot{E}_{x,in} = \sum \dot{E}_{x,out}, \quad (5)$$

If there is exergy storage ($\dot{E}_{x,dest}$) in the control region, Eq. (6) is written:

$$\sum \dot{E}_{x,in} - \sum \dot{E}_{x,out} = \sum \dot{E}_{x,dest}. \quad (6)$$

There is exergy entering ($\dot{E}_{x,mass,in}$), exiting ($\dot{E}_{x,mass,out}$) the control region, as well as exergy produced ($\dot{E}_{x,heat}$), workable ($\dot{E}_{x,work}$) and stored ($\dot{E}_{x,dest}$). In this case, the exergy flow in the control region is written as Eq. (7):

$$\dot{E}_{x,heat} - \dot{E}_{x,work} + \dot{E}_{x,mass,in} - \dot{E}_{x,mass,out} = \dot{E}_{x,dest}, \quad (7)$$

where in terms of exergy

$$\varepsilon_{in} = (h_{in} - h_o) - T_o\,(s_{in} - s_o), \quad (8)$$

$$\varepsilon_{out} = (h_{out} - h_o) - T_o\,(s_{out} - s_o). \quad (9)$$

Substituting Eqs. (8) and (9) into Eq. (7) yields

$$\left(1 - \frac{T_o}{T_{sun}}\right)\dot{Q}_{sun} - \dot{m}[(h_{out} - h_{in}) - T_o(s_{out} - s_{in})] = \dot{E}_{x,dest} \quad (10)$$

The enthalpy and entropy change of the flowing air in the collector are determined by [25]:

$$\Delta h = h_{out} - h_{in} = c_{p,air}\left(T_{air,out} - T_{air,in}\right), \quad (11)$$

$$\Delta s = s_{out} - s_{in} = c_{p,air}\ln\frac{T_{air,out}}{T_{air,in}} - R\ln\frac{P_{air,out}}{P_{air,in}}. \quad (12)$$

If Eqs. (1)–(12) are substituted in Eq. (10), it becomes

$$\left(1 - \frac{T_o}{T_{sun}}\right) I_T \tau\alpha A_{col} - \dot{m}c_{p,air}\left(T_{air,out} - T_{air,in}\right) + \dot{m}c_{p,air}\,T_o \ln\frac{T_{air,out}}{T_{air,in}} - \dot{m}RT_o\ln\frac{P_{air,out}}{P_{air,in}} = \dot{E}_{x,dest}. \quad (13)$$

The exergy loss and irreversibility of the system are

$$\dot{E}_{x,dest} = T_o\dot{S}_{gen}. \quad (14)$$

After determining the exergy gain and exergy loss irreversibility of the solar collector, the second law efficiency is written as equation (15). It is defined as the ratio of the useful exergy leaving the system to the total exergy entering the system:

$$\psi = \frac{\dot{E}_{x,out}}{\dot{E}_{x,in}} = \frac{\dot{m}\,[(h_{out} - h_{in}) - T_o(s_{out} - s_{in})]}{\left(1 - \frac{T_o}{T_{sun}}\right)\dot{Q}_{sun}} = \frac{\dot{m}\,c_p\left[(T_{out} - T_{in}) - T_o\ln\frac{T_{out}}{T_{in}}\right]}{\left(1 - \frac{T_o}{T_{sun}}\right)\dot{Q}_{sun}}. \quad (15)$$

4. Results and discussion

This study was carried out in the city of Çorum in Turkey. The solar air collector with two different flow surfaces was investigated as an experimental device. The collector is isolated from the bottom and the sides against the environment. The collector receives its energy from the sun. This energy is transferred to the air flowing through the corrugated panels. The temperature change values of the collector are explained in Fig. 4. The energy transfer ability determines the efficiency of the collector and is shown in Fig. 5.

Experimental values were measured in June and July. The ambient temperature was measured between 28°C and 35°C during the daytime. The design of both solar collectors is different, but the inlet temperatures are the same for both because the inlet airflow is connected to the same manifold. The outlet temperatures from the collectors are different. During the experiment, the highest inflowing air temperature was measured at 13 o'clock (31.8°C), see Fig. 4.

The more the air flow comes in contact with the surface of the corrugated panel heated by the sun, the more the temperature

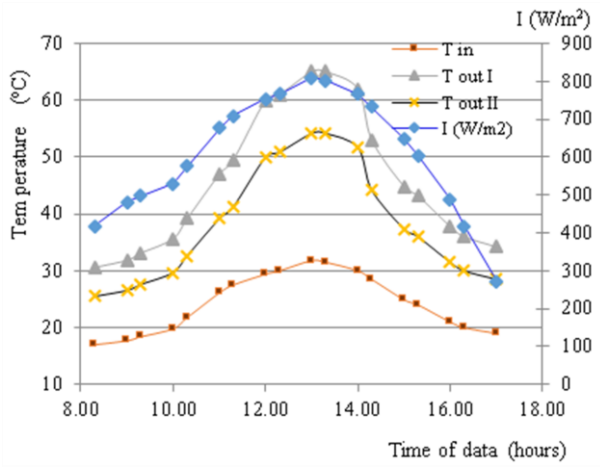

Fig. 4. The weather conditions and temperature increase across the solar air collectors on June14, 2021.

of the air increases. It may be good to keep the surface large in such collector systems, but large dimensions require larger space. Corrugated panels were created to increase the surface and reduce the length of the panel. By making zigzag rough surfaces inside the panel groove, the flow air is ensured to come into contact with the larger surface area.

The measured outflowing air temperatures in collector I and collector II are 65°C and 54.2°C, respectively. It is seen from Fig. 5 that the collector efficiency reaches its maximum values between the hours 08:30 and 17:00.

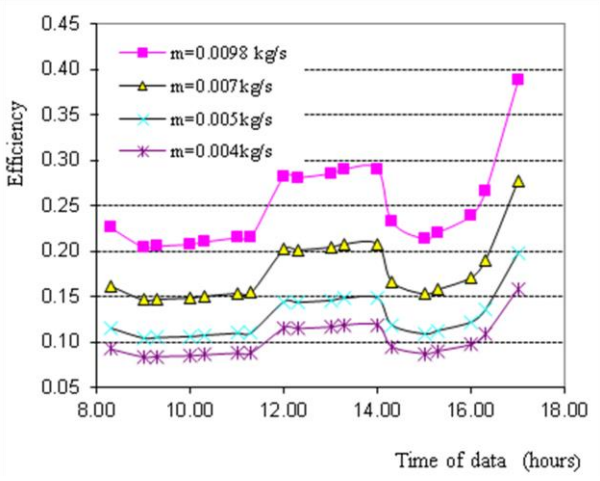

Fig. 5. Efficiency versus time of day in collector I.

The panel efficiency of the fan was observed at four different flow rates. The collector efficiency is maximum at the value of air mass flow $\dot{m}$ = 0.0098 kg/s. In the case of mass flow rate $\dot{m}$ = 0.004 kg/s, collector I's exergetic efficiency is very low. As the air flow rate decreases, the second law efficiency of the panel also decreases.

Karim and Hawlader [26] conducted an experimental study of three types of solar air collectors under Singapore climatic conditions. These collectors have flat plates, fins and V-grooves. It was found that the V-groove collector is the most efficient collector, while the flat plate collector is the least efficient collector. It was also shown that the V-slot collector has a 7−12% higher efficiency than the flat collector.

As seen from Fig. 6, when the inlet and outlet air temperature difference is compared for the same radiation values of both panels, the air temperature difference is higher in collector I.

Radiation values and temperature input-output values of both panels were compared. It is understood that at the same radiation values, the inlet-outlet temperature difference in collector I is higher. The reason for this is that there is a zigzag strip inside the panel.

In Fig. 7, changing radiation values were observed while keeping the flow rate and input temperature of air constant for both collectors. According to the second law, the exergetic efficiency of collector I, which has a zigzag inside the panel, is between 20.2% and 38.8%. It was concluded that the exergetic efficiency of collector II, which is hollow inside the panel, varies between 17% and 32.2%. In both collectors, the highest efficiency was obtained when the ambient temperature was lower.

As seen in Fig. 8, when the solar radiation reaches its maximum at 13:00, the exergetic efficiencies of both collectors reach its maximum at 29.8% for collector I and 24.8% for collector II. Although exposed to the same radiation, the exergetic efficiency of collector I is higher than that of collector II.

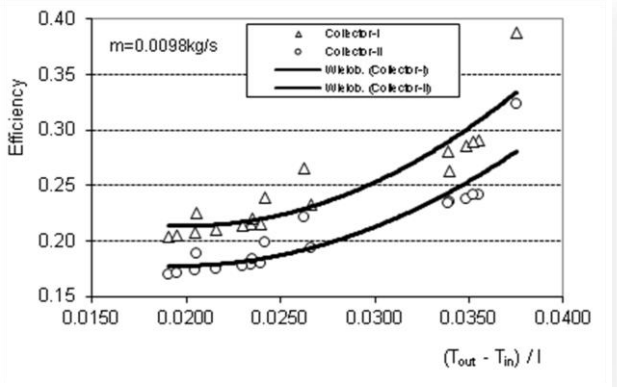

Fig. 7. Variation of collector efficiency versus parameter $(T_{out} - T_{in})/I$ at mass flow rate 0.0098 kg/s for different types of absorber plates.

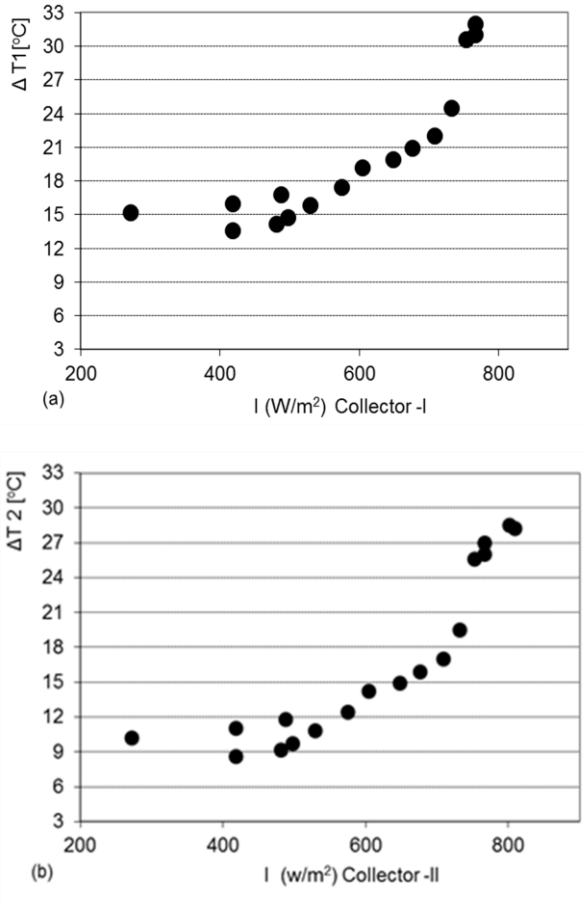

Fig. 6. Variation of temperature difference with incident radiation.

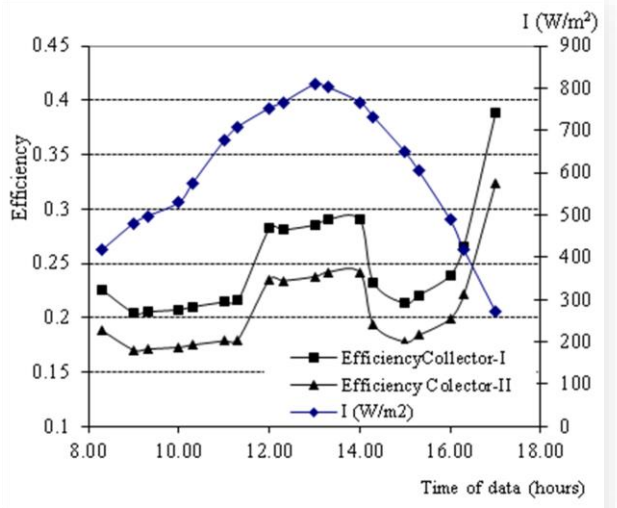

Fig. 8. The productivity changes of collector I and collector II at different radiation values.

The Ansys programme [27] was used for the display of floe parameters in the panel. The programme outputs are shown in Figs. 9−11. The air flow was observed with the highest values at the inlet and outlet of the panels (Fig. 9). It is seen in Fig. 10 that the pressure inside the panel grooves is lower than in the collector inlet–outlet. This is due to the pressure formation against the air flow inside the groove panels. Vortex changes inside panels can be seen in Fig. 11.

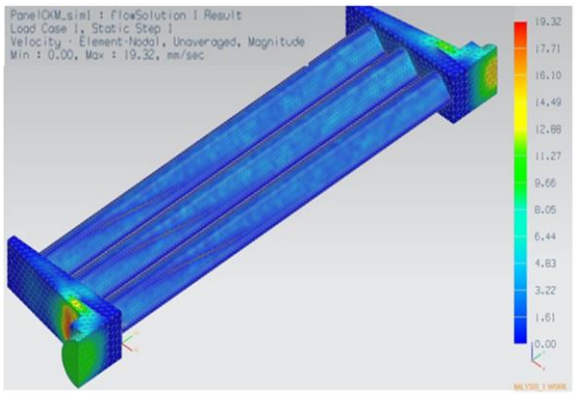

Fig. 9. Full width figure example: Panel I CKM sim l; flow Solution 1 Result; Load case 1; Static step 1; Velocity – element nodal, unaveraged, magnitude: min 0.00, max 19.32 mm/sec.

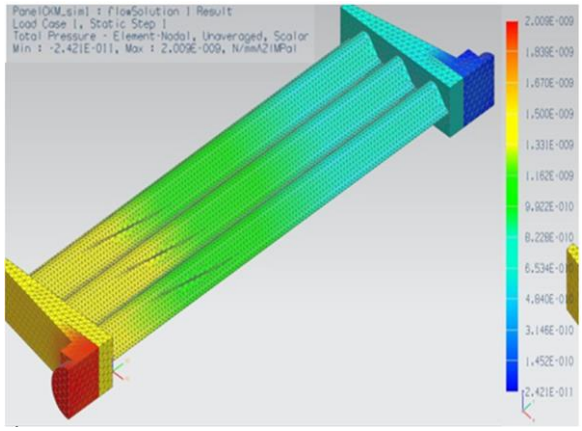

Fig. 10. Flow pressure change along the channel: Panel I CKM sim l; flow Solution 1 Result; Load case; Static step 1; Total pressure – element nodal, unaveraged, scalar: min $2.42I^{-011}$, max 2.009^{-009} N/mm^2 (MPa).

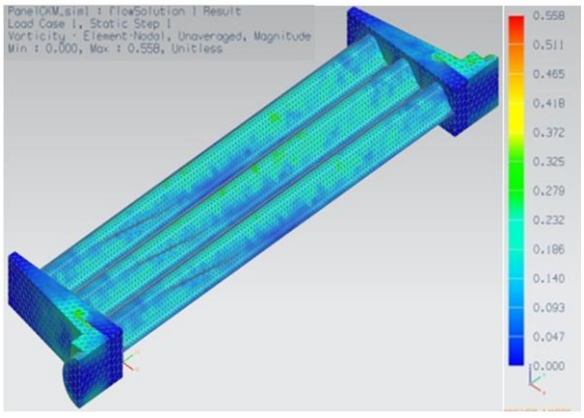

Fig. 11. Vortex along the channel change: Panel 1 CKM sim l: flow Solution 1 Result; Load Case 1; Static step 1; Vorticity – element nodal, unaveraged, magnitude: min 0.00, max 0.558 (unitless).

5. Conclusions

This study aims to investigate the effect of using various fin arrangements inside a corrugated panel with a solar thermal source. The study experiments were carried out in Corum in June–July. The experiment was carried out between 8:30 and 17:00 and the thermodynamic parameters were measured and recorded. Under the same conditions, the air temperature leaving collector I was higher than that of collector II. The highest exit temperature was reached at 13:00 in both collectors and is graphed in Fig. 4. Another important parameter for both collectors is the amount of air flow passing through the collector grooves. The collector efficiency analysis was carried out by considering the changes in these air flow amounts. The air flow was measured from Collector I between 11:00 and 15:00, at approximately 54.2ºC and 65ºC. The results presented in this study show that the efficient fin arrangement has a great effect on the heat energy transfer performance of the plate. A zig-zag fins placed inside the corrugated panel show that heat transfer is significantly improved.

References

[1] Abene, A., Dubois, V., Le Ray, M., & Ouagued, A. (2004). Study of a solar air flat plate collector use of obstacles and application for the drying of grape. *Journal of Food Engineering*, 65(1), 15– 22. doi: 10.1016/j.jfoodeng.2003.11.002

[2] Zıma, W., & Dzierwa, P. (2010). Mathematical modelling of heat transfer in liquid flat-plate solar collector tubes. *Archives of Thermodynamics*, 31(2), 45–62. doi: 10.2478/v10173-010-0008-7

[3] Krawczyk, P. (2013). Cumulative ventilation air drying potential as an indication of dry mass content in wastewater sludge in a thin-layer solar drying facility. *Archives of Thermodynamics*, 34(4), 23–34. doi: 10.2478/aoter-2013-0027

[4] Khatri, R., Goswami, S., Anas, M., Sharma, S., Agarwal, S., & Aggarwal, S. (2020). Performance evaluation of an arched plate solar air heater with porous aluminum wire mesh cylindrical fins. *Energy Reports*, 6(9), 627–633. doi: 10.1016/j.egyr.2020.11.177

[5] El-Khawajah, M.F. Aldabbagh, L.B.Y., & Egelioglu, F. (2011). The effect of using transverse fins on a double pass flow solar air heater using wire mesh as an absorber. *Solar Energy*, 85(7), 1479–1487. doi: 10.1016/j.solener.2011.04.004

[6] Sharma, S., Kumar, D.R., & Kulkarni, K. (2021). Computational and experimental assessment of solar air heater roughened with six different baffles. *Case Studies in Thermal Engineering*, 27, 101350. doi:10.1016/j.csite.2021.101350

[7] Petela, R. (2003). Exergy of undiluted thermal radiation. *Solar Energy*, 74(6), 469–488. doi: 10.1016/S0038-092X(03)00226-3

[8] Sivakumar, V., & Sundaram, G.E., (2016). MATLAB modelling and examination of the effect of heat capacity of basin and glass cover on performance of solar still by thermal models. *International Journal of Ambient Energy*, 39(1), 1–10. doi: 10.1080/01430750.2016.1222956

[9] Farahat, S., Ajam, H., & Sarhaddi, F. (2004). Method and basis of flat plate collector optimization with exergy concept. *Proceedings of First Iranian Conference on Ecoenergy*, Urmia, Iran.

[10] Çomakli, Ö., & Yüksel, F. (1994). Experimental investigation of the exergetic efficiency of air heating flat-plate solar collector with distorted plates. *Energy Conversion and Management*, 35(2), 121–126. doi: 10.1016/0196-8904(94)90072-8

[11] Karsli, S. (2007). Performance analysis of new-design solar air collectors for drying applications. *Renewable Energy*, 32(10) 1645–1660. doi: 10.1016/j.renene.2006.08.005

[12] Altfeld, K., Leiner, W., & Fiebig, M. (1988). Second law optimization of flat-plate solar air heaters Part I: The concept of net exergy flow and the modeling of solar air heaters. *Solar Energy*, 41(2), 127–32. doi: 10.1016/0038-092X(88)90128-4

[13] Altfeld, K., Leiner, W., & Fiebig, M. (1988). Second law optimization of flat-plate solar air heaters Part 2: Results of optimization and analysis of sensibility to variations of operating conditions. *Solar Energy*, 41(4), 309–317. doi: 10.1016/0038-092X(88)90026-6

[14] Gupta, M.K., & Kaushik, S.C. (2008). Exergetic performance evaluation and parametric studies of solar air heater. *Energy*, 33(11), 1691–702. doi: 10.1016/j.energy.2008.05.010

[15] Dincer, I., & Rosen, M.A. (2008). *Thermal Energy Storage: Systems and Applications*. Wiley & Sons, New York.

[16] Esen, H. (2008). Experimental energy and exergy analysis of a double-flow solar air heater having different obstacles on absorber plates. *Building and Environment*, 43(6), 1046–1054. doi: 10.1016/j.buildenv.2007.02.016

[17] Bejan, A. (1988). *Advanced Engineering Thermodynamics* (2nd ed.) (pp.133–137 & 462-465). Wiley & Sons.

[18] Wark Jr., K. (1997). *Advanced Thermodynamics for Engineers*. McGraw-Hill, New York.

[19] Ucar, A., & Inalli, M. (2006). Thermal and exergy analysis of solar air collectors with passive augmentation techniques. *International Communications in Heat and Mass Transfer*, 33(10), 1281–1290. doi: 10.1016/j.icheatmasstransfer.2006.08.006

[20] Akpinar, E.K., & Kocyigit, F. (2010). Energy and exergy analysis of a new flat-plate solar air heater having different obstacles on absorber plates. *Applied Energy*, 87(11), 3438–3450 doi: 10.1016/j.apenergy.2010.05.017

[21] Sivakumar, V., Sundaram, E.G., & Sakthivel, M. (2016). Investigation on the effects of heat capacity on the theoretical analysis of single slope passive solar still. *Desalinational and Water Treatment*, 57(20), 9190–9202. doi: 10.1080/19443994.2015.1026284

[22] Kaushik, S.C., Abhyankar, Y.P., Bose, S., & Mohan, S. (2001). Exergoeconomic evaluation of a solar thermal power plant. *International Journal of Solar Energy*, 21(4), 293–314. doi: 10.1080/01425910108914377

[23] Yousef, M., Hassan, H., Ahmed, M., & Ookawaraa, S. (2017). Energy and exergy analysis of single slope passive solar still under Egyptian climate conditions. *Energy Procedia*, 141, 18–23. doi: 10.1016/j.egypro.2017.11.005

[24] Torres-Reyes, E., Navarete-Gonzales, J.J., Zaleta-Aguilar, A., & Cervantes-De Gurtari, J.G. (2001). Exergy analysis of irreversible flat-plate solar collectors. *ECOS '01, The International Congress on Efficiency, Costs, Optimization, Simulation and environmental aspects of energy systems and processes*, July 4–6, Istanbul, Turkey.

[25] Cengel, Y.A., & Boles, M.A. (2006). *Thermodynamics: An Engineering Approach* (5th ed.). McGraw-Hill, New York.

[26] Karim, M.A., & Hawlader, M.N.A. (2004). Development of solar air collectors for drying applications. *Energy Conversion and Management*, 45(3), 329–344. doi: 10.1016/S0196-8904(03)00158-4

[27] http://www.ansys.com